Influence of the initial structure on the efficiency of laser processing of steel

G. I. Brover · E. E. Shcherbakova

Received: 31 August 2023 / Revised: 9 November 2023 / Accepted: 5 January 2024 / Published online: 19 June 2024

Abstract
According to experiments, the initial martensitic structure with inherent carbon content is most suitable for high-speed laser hardening during preliminary volumetric heat treatment, releasing a suitable amount and dispersion of carbides during tempering. When choosing a volumetric heat treatment mode, it is necessary to consider that the α→γ transformation during laser heating occurs via a shear mechanism with the hereditary transfer of carbon atoms and alloying elements, as well as defects in the crystal structure, to austenite from the original martensite. High-temperature laser-hardened austenite has a fragmented structure with subgrains 200–300 nm in size. This feature is due to the dynamic polygonization of austenite, which occurs because of the superposition of dynamic thermostrictive effects in the laser processing zones on phase hardening during the α→γ transition. After high-speed cooling, the irradiated zones contain hereditary fine-needle martensite with high-strength properties, a certain amount of textured residual austenite, and a carbide phase. It has been established that the strengthening of irradiated steel, which occurs under conditions of thermal deformation of laser radiation, is associated, among other things, with the formation of nanosized zones at the carbide steel matrix composition interface, which have a dispersed structure and increased hardness (10–12 GPa). Metallophysical and urometric studies showed that the maximum hardness of laser-hardened steels is achieved if dispersed carbides occupy more than 40% of the irradiated area and have dimensions of 0.5–1.5 μm. A reasonable choice of the initial steel structure and laser processing mode enabled obtaining a structural state of surface layers on the working surfaces of products having high and predictable performance properties.

Keywords Laser processing · Steel · Structure · Properties

Introduction

According to [1–4], the locality of laser processing, combined with high heating and cooling rates, lack of exposure at the heating temperature, and high-temperature gradients, leads to the emergence of thermostrictive stresses and local plastic deformations in the irradiated materials, which are of greatest importance in the structure formation and hardening of steel surfaces.

Extreme laser processing conditions shift the critical temperatures of phase transitions; austenitization during heating occurs through a shear mechanism. Moreover, high-speed laser heat treatment allows for separating the stages of the steel recrystallization process, namely, phase α→γ transformation and recrystallization of phase-hardened austenite.

Translated from *Metallurg*, No. 2, pp. 30–37, February, 2024. Russian DOI: https://doi.org/10.52351/00260827_2024_2_30

Notably, the dissolution of excess carbides during laser irradiation is considerably limited. Homogenization processes partially develop even when the metal surface melts. In solid solutions, high-concentration heterogeneity remains. Moreover, under the thermal deformation conditions of laser processing, the final structure of steel is determined by the superposition of the level of stresses arising in the zones of laser irradiation and the degree of energy dissipation processes due to local plastic deformation, dynamic recovery, polygonization, and early stages of recrystallization [5].

In this work, the degree of preparedness of a steel structure for high-speed laser hardening was assessed to obtain the highest possible homogeneity of the hardened surface layer of steel. A reasonable choice of the initial structure and energy regime of laser heating of steels allows for obtaining various structural compositions in the surface layers of irradiated products and isolating those compositions that are preferable to ensure specified performance properties.

Research method

Analysis of structure formation processes under high-speed laser heating was performed on samples of commercial iron with a relatively homogeneous ferrite structure, annealed hypoeutectoid steel 45 with a ferrite-pearlite structure, and U8 eutectoid steel after annealing (with a lamellar pearlite structure) and volumetric hardening to a martensitic structure. The materials used in this study also included samples of R6M5 alloy steel after volumetric hardening and tempering at different temperatures.

Pulsed laser irradiation was performed using a Kvant-16 technological unit. Changes in the radiation energy, the degree of beam defocusing (3–6 mm), and the duration of the radiation pulse $(1–6)\cdot10^{-3}$ s enabled us to vary the radiation power density over a wide range (70–200 MW/m^2), i.e., irradiation was performed without and with melting of the surface of the samples.

Metallophysical experiments were performed on samples $10\times10\times20$ mm in size. Identification of the phase composition and study of the structure of materials after laser processing were performed using several methods, namely, metallography, X-ray spectroscopy, scanning probe microscopy, and hardness measurements.

Metallographic studies were conducted on transverse and longitudinal sections using MIM-7 and Neophot-21 microscopes. A DRON-0.5 diffractometer was used for the X-ray diffraction analysis. Microhardness measurements were performed on a PMT-3 device with a load of 0.49 N.

Experimental results and discussion

When considering the features of structure formation during high-speed laser heat treatment of steels, starting with almost single-phase (ferritic) technical iron, it should be noted that under conditions of high-temperature gradients and thermostrictive stresses, local plastic deformations may appear in the irradiated zones of the metal, affecting the formation processes of the structures.

During metallographic studies of technical iron samples after thermal deformation laser treatment, traces of local plastic deformation of the metal in the irradiation zones were discovered (Fig. 1b). To obtain and identify these imprints, prepolished and etched transverse sections of technical iron with microhardness tester indenter imprints as reference points (Fig. 1a) were subjected to laser irradiation along the sample surface perpendicular to the section.

With repeated etching on transverse sections (Fig. 1b), ferrite grain boundary (ribbon boundary) migration is noted with a certain orientation of the boundary shift process. The indenter imprints of the microhardness tester are also distorted.

The result obtained is a consequence of the relaxation of thermostrictive stresses arising in the irradiated zones of materials [6].

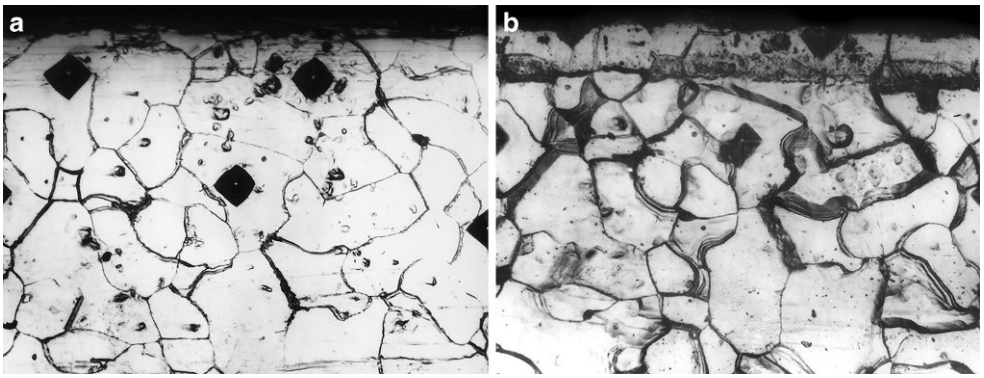

Fig. 1 Microstructure of technical iron before (**a**) and after (**b**) laser processing

To substantiate and confirm the possibility of deformation and relaxation processes in the irradiated zones of the metal under high-speed laser processing, the approximate level of shear stresses causing plastic deformation in the surface layers of commercial iron was determined [7].

It was assumed that during plastic deformation, dislocations are displaced by the formation of slide lines or stripes and relief grain boundaries on the irradiated surface. The magnitude of the resulting displacement is proportional to the value of nb, where n is the number of dislocations reaching the surface, and b is the Burgers vector of the material.

In the calculations, it was assumed that the elastic deformation in the crystal preceding sliding can be defined as τ/G, where τ is the applied stress, and G is the shear modulus of the material. However, it is necessary to consider that elastic deformation during sliding can relax in a region with a diameter of $2L$, where L is the length of the dislocation slide lines [7].

Assuming that there has been a complete transition from elastic deformation ($2L\tau/G$) to plastic deformation, equal to the nb value when n dislocation loops propagate, we obtain the following expression:

$$nb = 2L\tau/G,$$

where $n = 40$–70 is the number of slide lines in one grain, with $l_{\text{grain}} \approx 10^{-6}$ m [8]; $b = 2.48 \cdot 10^{-10}$ is Burgers vector (for iron), m; $G = 6.4 \cdot 10^4$ is shear modulus (for iron), MPa; and L is the length of dislocation slide lines (we take $L = 10^{-3}$ mm [8]).

According to the calculation, the shear stress τ, which causes plastic deformation, is 317.44–555.5 MPa for technical iron and substantially exceeds the conventional yield strength of iron, which is equal to 100–120 MPa.

An assessment was also made of the degree of residual plastic deformation ε_{sc}, which ranged from 5 to 9%.

Stress and plastic deformation in local areas of metals arising during the action of a powerful thermal shock of a laser pulse will undoubtedly have much greater values in actuality.

Thus, the magnitude of the shear stresses acting in the irradiated zones of the metal is sufficient not only to cause local plastic deformation of the metal but also to initiate processes of partial relaxation of deformation effects through the dynamic processes of polygonization and recrystallization.

In Fig. 2a, the results of the relaxation of dynamic effects are recorded in the form of considerable refinement of the ferrite grain on transverse sections of iron (without preliminary etching).

The ferrite grain size (Fig. 2b) decreased to 0.5–10 µm compared to the underlying main structure with a grain of 35–80 µm. The microhardness in the fine grain zone is 2–2.5 GPa compared to 1.0–1.2 GPa in the initial metal.

In this case, the pattern of structural transformations during laser heating can be presented as follows.

The initial stages of austenite formation during high-speed heating of iron samples are implemented by the shear $\alpha \rightarrow \gamma$ mechanism [9, 10].

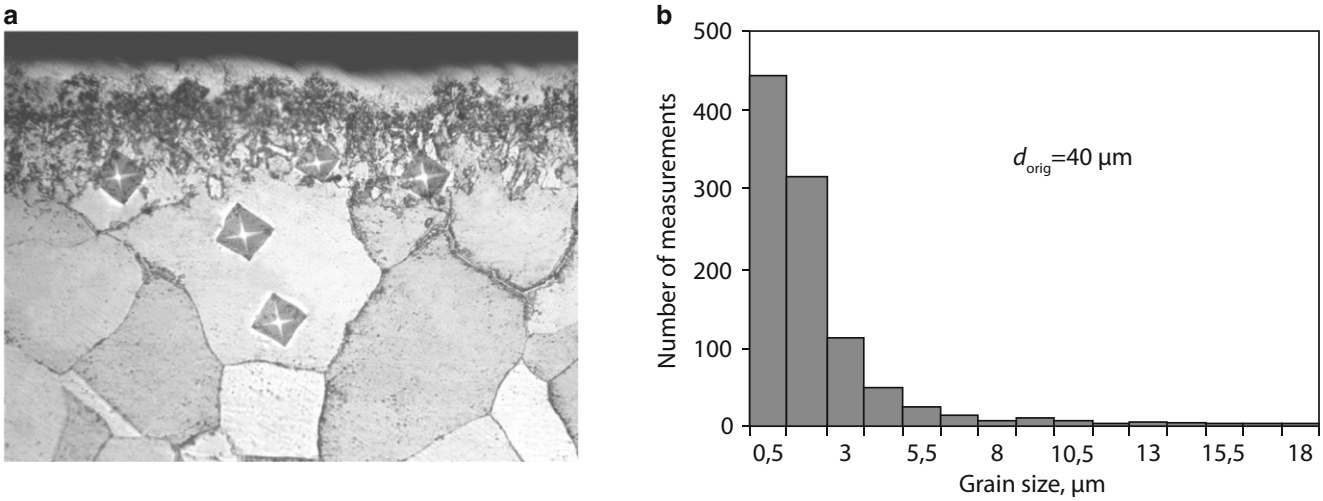

Fig. 2 Microstructure of the irradiated technical iron (**a**) and histogram of the grain size distribution (**b**)

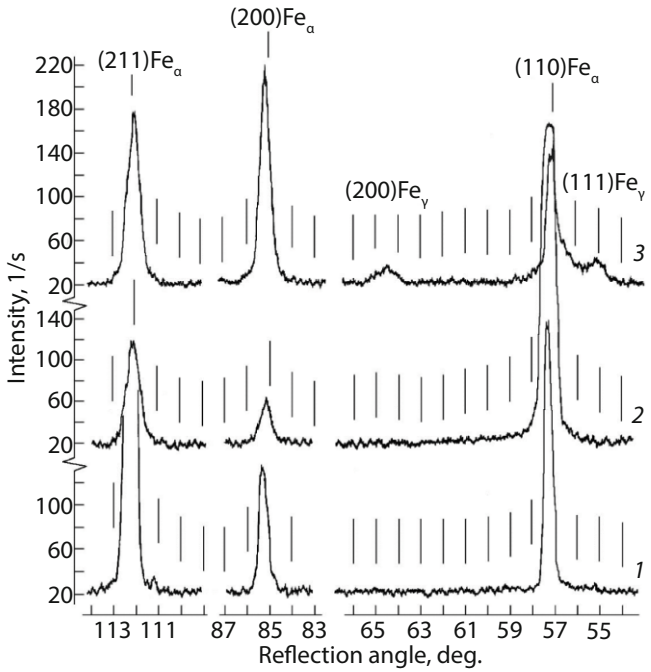

Fig. 3 Fragments of the diffraction patterns of technical iron: *1* in the initial state; *2* laser hardening without melting; *3* with surface melting

In the resulting austenite phase-hardened during recrystallization, high-temperature dynamic polygonization occurs under conditions of the temperature-deformation action of laser radiation, which contributes to the creation of a developed substructure with low-angle boundaries [11].

The fragmented structure of hot-deformed austenite in laser processing zones is hereditarily transferred to the α-phase during the reverse shear γ→α transformation with subsequent recrystallization, leading to the formation of a fine-grained structure [12, 13].

The peculiarities of the course of the structure formation processes under consideration are confirmed by the results of the X-ray diffraction studies presented in Fig. 3.

Because of the laser irradiation of technical iron samples, the *a*-phase reflections broaden and shift to small angles. For example, the width of the (211) reflection of the α-phase increases from $B = 07364$ mrad in the initial state (Fig. 3, curve *1*) to $B = 1.5976$ mrad after laser treatment from the solid (austenitic) state (Fig. 3,

https://doi.org/10.1007/s11015-024-01715-4

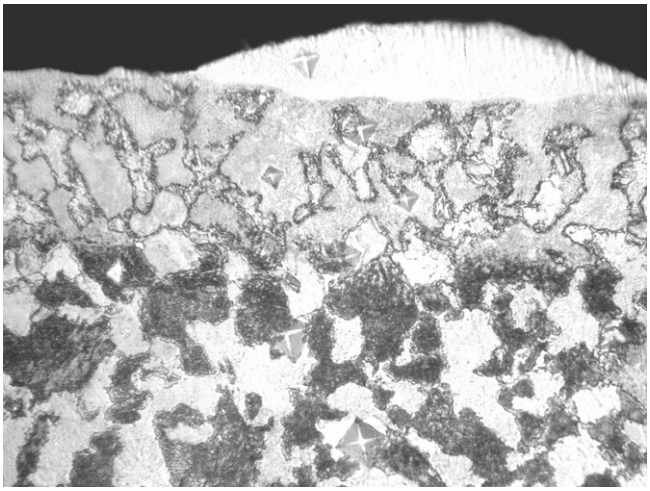

Fig. 4 Microstructure of steel 45 after laser heat treatment

curve *2*), i.e., without melting the iron surface. A shift of this reflex to smaller reflection angles is also noted (from 112.302° before laser irradiation to 112.1358° after it).

These results are associated with the formation of a dispersed, practically carbon-free α-phase (carbon-free martensite) with a high dislocation density in the laser hardening zone.

Notably, during the laser melting of the surface (Fig. 3, curve *3*), weak reflections of the γ-phase are recorded on the X-ray diffraction patterns despite the unsubstantial carbon content in the technical iron. These reflections may have several causes. First, the dissolution of tertiary cementite in liquid metal changes its chemical composition and somewhat lowers the points of polymorphic (martensitic) transformation. The inhibition of shear during the γ→α transformation can be facilitated by the high density of defects in the crystal structure of hot-deformed austenite in the irradiated material.

An increase in the intensity of the reflection (200) of the α-phase is clearly visible in curve *3* (Fig. 3) and evidence of the formation of texture effects during laser melting. These structural changes increase the properties of technical iron in the irradiated zones.

Additional information on structure formation during high-speed heat treatment is provided by studies of steel 45, whose initial structure before irradiation, in addition to ferrite grains, contains lamellar pearlite grains. While discussing the experimental results, it was considered that during high-speed laser heating of steels, austenite formation occurs under conditions far from equilibrium, when the diffusion of carbon atoms is difficult. Therefore, austenite can form independently and almost simultaneously in the pearlite and ferrite sections of the structure. Consequently, the γ-phase can have a very heterogeneous carbon composition after the end of austenitization.

The microstructure of steel 45 after laser treatment, illustrating the resulting structural heterogeneity, is presented in Fig. 4.

In the irradiated layer, etching revealed a hardening zone from the liquid state. This zone has a uniformly dispersed structure, a light, inhomogeneous hardening zone from the solid state, and a ferrite–pearlite structure of the base metal.

In the laser heating zone from the solid state, austenitization in the field of ferrite spaces occurs through the structural transformations described above for ferrite grains of technical iron, i.e., in the ferritic grains of steel 45, a structure of carbon-free martensite is formed during laser processing. The hardness of the ferrite grains increases to 2.0–2.5 GPa.

Structural transformations in pearlite grains during laser irradiation of steel 45, and in U8 steel with a completely pearlite structure, are of particular interest.

It has been suggested that during laser heating of pearlite areas of the steel structure, elastic stresses may arise at the interfaces of the cementite–ferrite composition. This result is observed because the thermal expansion

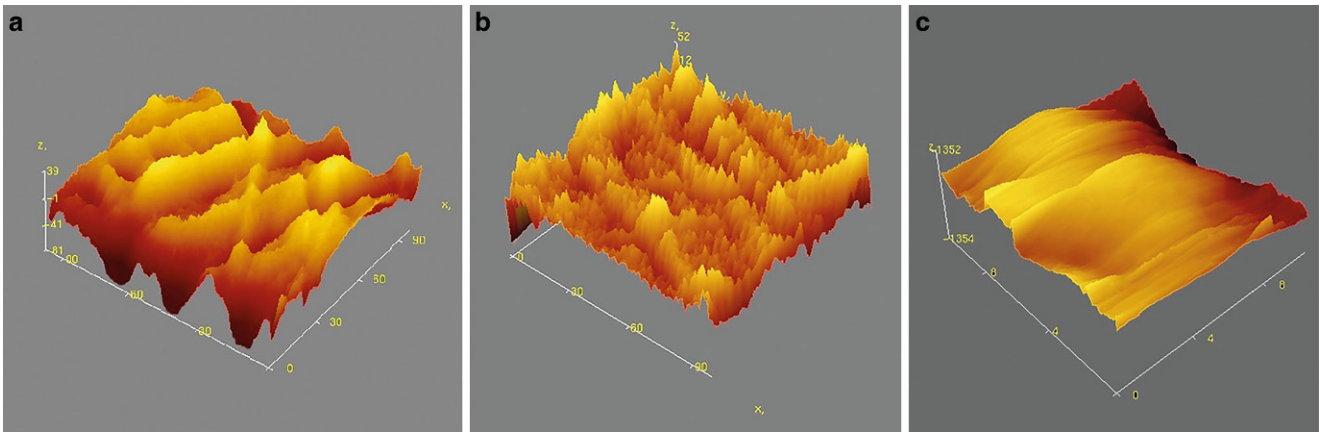

Fig. 5 Structure of U8 steel before irradiation (lamellar pearlite) (**a**), after laser processing without melting (**b**), and with surface melting (**c**)

coefficient of cementite is considerably lower than that of iron. The relaxation of these stresses along with the fields of thermostrictive stresses formed in the surface layers of steel under the influence of high temperatures and heating rates is accompanied not only by the dynamic polygonization of austenite in place of former ferrite plates but also by the formation of thin, several nanometers thick, interlayers of liquid metal at interphase boundaries in the cementite–polygonized austenite system (contact melting effect) [14, 15].

Liquid interlayers actively absorb carbon from cementite inclusions and enrich nearby thin austenite zones with it. After high-speed cooling, martensite, which is heterogeneous in carbon content, is formed between the remnants of cementite plates of pearlite.

The possible partial near-boundary dissolution of cementite plates in pearlite grains was determined by studying irradiated steels 45 and U8 using scanning probe microscopy (SPM) (Fig. 5).

In the zones of laser processing without surface melting (Fig. 5b), cementite peaks with a complex defect structure are noted against the background of martensite layers that are heterogeneous in composition and properties. The height of the cementite plates was 170–350 nm and 70–130 nm before and after laser irradiation, respectively (Fig. 5a).

For comparison, Fig. 5c illustrates the structure of U8 pearlitic steel after laser melting of the sample surface. The metal matrix has almost completely melted, retaining some carbides in a semidissolved state. In this case, during high-speed cooling, crystallization occurs with the formation of a finely dispersed dendritic structure (75–175 nm), whose size and orientation depend on the heat removal rate.

It can be concluded that U8 steel and pearlite grains of steel 45 irradiated without surface melting have the form of a conglomerate of slightly dissolved cementite plates and martensite, which is heterogeneous in carbon concentration. The irradiated zones have an average hardness of 8.0–8.5 GPa (Fig. 6), corresponding to the hardness of bulk-hardened steel.

The possible occurrence of the above structure formation processes in irradiated annealed steels is evidenced by the X-ray diffraction analysis results of U8 steel (Fig. 7).

To process the results of the diffractometric studies, we used the "New_Profile" package of modern software, which can be used to separate the complex profile of the overlapping diffraction reflections of the phases.

As seen in Fig. 7a, after laser irradiation, the reflections of the α- and γ-phases are recorded (Fig. 7b, reflection *1*), and the separation of martensite reflections by carbon content into carbon α- (Fig. 7b, reflection *2*) and low-carbon χ-martensite (Fig. 7b, reflection 3) is noted.

The reflection of low-carbon χ-martensite is located at angles 2θ of 57.0801°, the interplanar distance is 2.02603 Å, and the width of the reflection is $B = 2.00025$ mrad. The reflection of carbon α-martensite is at angles $2\theta = 56.1400°$, has an interplanar distance equal to 2.05714, and B is 1.09629 mrad.

https://doi.org/10.1007/s11015-024-01715-4

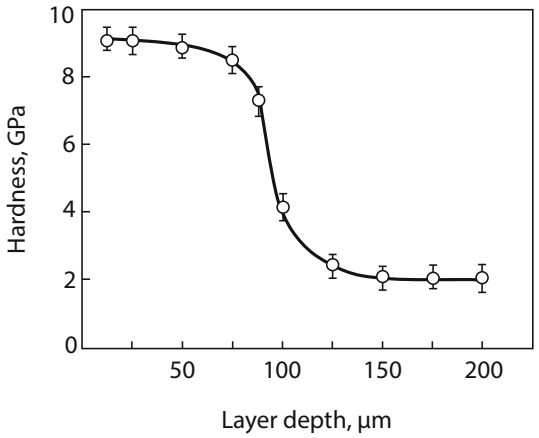

Fig. 6 Hardness distribution along the depth of the laser-hardened layer on the annealed U8 steel

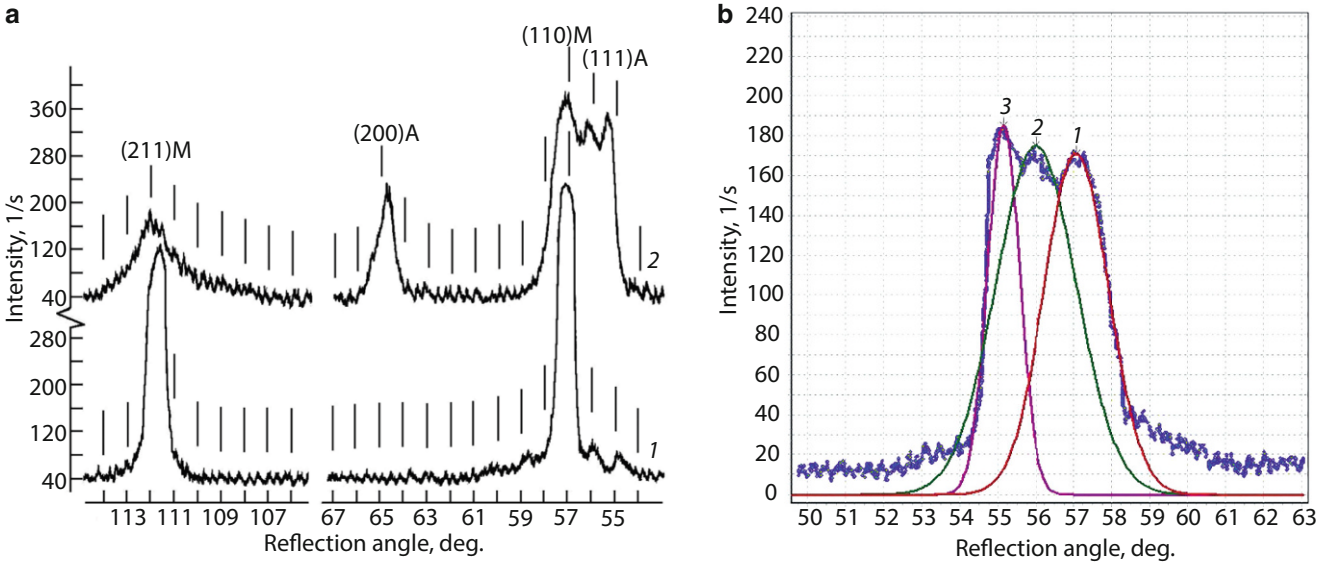

Fig. 7 Fragments of X-ray diffraction patterns of U8 steel: **a** after annealing (curve *1*) and subsequent laser hardening from the solid state (curve *2*); **b** processing the results of X-ray structural studies in the "New_Profile" program

The results obtained confirm the validity of the proposed model of structure formation in annealed steels during high-speed heating in the absence of time for diffusion processes to occur.

Contact melting of interphase boundaries can also explain the accelerated mass transfer of carbon atoms and alloying elements from carbides (cementite) to nearby matrix zones through the liquid phase for alloy steels [16, 17].

The above results indicate a high structural and concentration inhomogeneity of the laser hardening zones with the initial annealed structure of U8 steel and particularly steel 45.

The resulting ensembles of structurally inhomogeneous sites do not allow for unambiguous predictions of the operational properties of irradiated products. Apparently, the initial structure, which can transform into a high-temperature γ-phase via a shear-diffusion-free mechanism with hereditary transmission of carbon content and defects in the crystal structure of the initial α-phase, should be considered the most suitable for high-speed laser hardening [18]. The γ-phase formed under conditions of high-speed laser heating acquires a fragmented structure due to the occurrence of dynamic polygonization caused by the combined effect of phase hardening during the α→γ transformation, as well as dynamic effects arising under the influence of thermal stresses in the irradiated zone. During high-speed cooling, the listed processes will ensure the production of fine-crystalline

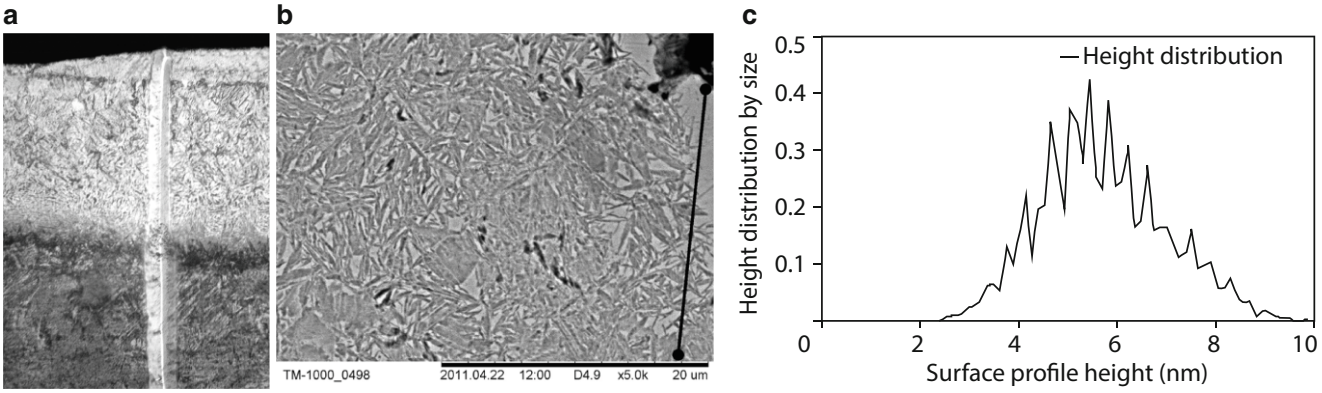

Fig. 8 Microstructure of the laser hardening zone on U8 steel after volumetric heat treatment (**a**); structure of martensite during laser hardening of U8 steel (SPM) (**b**); and distribution of heights of the profile of martensite needles (**c**)

products of shear γ→α transformation and possibly be a reason for preserving, if necessary, a certain (specified) amount of transformation-resistant retained austenite.

Obviously, these requirements are met by the initial structure of martensite with the inherent carbon content during the preliminary volumetric heat treatment.

Notably, the quantity and degree of dispersion of the carbide phase in the initial structure before irradiation of the steel are also important. Let us consider in more detail the effect of the laser hardening process on the efficiency of the initial martensitic structure of steel and carbides obtained during tempering at different temperatures after volumetric hardening.

The studies were conducted using U8 carbon steel and R6M5 alloy steel subjected to volumetric hardening and tempering. Metallographic analysis of U8 carbon steel irradiated after volume heat treatment showed that the laser-hardened layer has a relatively uniform structure and a uniform change in hardness over depth, which is clearly visible in Fig. 8a along the width of the scratch of the microhardness tester indenter.

Studies of laser processing zones using electron microscopy (Fig. 8b) showed that martensite needles were refined (Fig. 8c) to an average transverse size of 5.5 nm. The above statements are also illustrated by the X-ray structural analysis results of U8 carbon steel after laser processing (Fig. 9a, curve *2*) and after the initial volumetric hardening (Fig. 9a, curve *1*).

According to Fig. 9a, after laser hardening, the α- and γ-phases have a large linewidth. The blurring of the diffraction lines in the X-ray diffraction patterns is due to the merging of doublets of the tetragonality of the martensite lattice, the inhomogeneity of the α-solid solution, the small size of the coherent scattering regions, and distortions in the lattice microvolumes.

The doublet of tetragonality that appears in the (211) reflection of the α-phase indicates a rather high content of carbon atoms in martensite, and consequently, the strengthening of the surface layers of steels during laser hardening.

The division of the multiple line (211) reflection of martensite in the "New_Profile" program is presented in Fig. 9b. The martensite lattice parameters are $a = 2.8637$ Å and $c = 2.9239$ Å, and the degree of lattice tetragonality is 1.0210, corresponding to an average carbon content of 0.45% in the martensite lattice. The lower carbon content values may be due to the high-speed of the laser irradiation process and the short homogenization time in the hardening zones.

To further develop the presented considerations on the influence of the initial structure of steel on the effect of laser hardening, experiments were performed on the irradiation of R6M5 alloy steel subjected to volumetric heat treatment in various modes (with varying tempering temperatures). Figure 10 presents the average statistical data on the depth (Fig. 10a) and hardness (Fig. 10b) of the laser-irradiated layers on the studied samples.

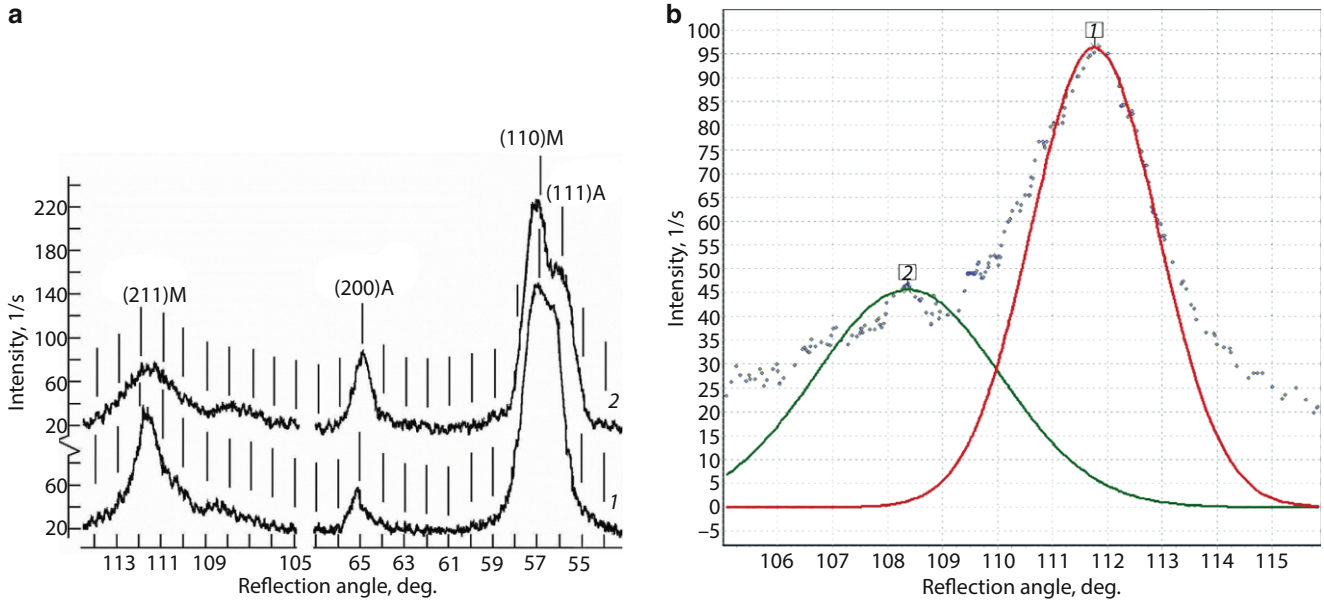

Fig. 9 Fragments of X-ray diffraction patterns of U8 steel after volumetric hardening (**a**, curve *1*), laser irradiation of volumetric heat-treated samples (**a**, curve *2*), and separation of the reflection doublet (211) M of U8 steel after laser processing in the "New_Profile" program (**b**)

As can be seen, the depth and hardness of the irradiated steel, previously subjected to volumetric hardening, considerably exceed those obtained by laser processing of steel after its annealing.

The best combination of the depth of the hardened layer and its hardness is achieved by laser irradiation of the initial structure comprising tempered martensite and dispersed alloyed carbides. This structure on R6M5 steel is obtained after volumetric heat treatment according to standard conditions, i.e., after quenching and tempering at 550–570 °C.

In this case, as shown by the results of the metallographic and urometric studies of the laser-hardened metal, carbides occupy at least 40% of the irradiated area of the steel and have dimensions of 0.5–1.5 μm (Fig. 11).

In this case, the increase in the hardness of the irradiated steel is explained by the formation of nanosized zones with a dispersed structure and increased hardness (10–12 GPa) during pulsed laser irradiation without melting the surface around carbide inclusions under the influence of thermal deformation stresses at the boundaries of the carbide steel matrix composition [19, 20].

It has been experimentally established that through a reasonable choice of the steel preliminary heat treatment mode and the parameters of the laser irradiation mode, the identified features of the structural state of the irradiated surface layers of steels enable obtaining a high level of performance properties in the surface layers of hardened products.

Conclusions

- It has been experimentally established that the initial martensitic structure with the carbon content inherent in it during preliminary volumetric heat treatment, as well as the amount and dispersion of carbides released during the tempering process, is most suitable for high-speed laser hardening.
- When choosing a volumetric heat treatment mode, it is necessary to consider that the α→γ transformation during laser heating occurs with a shear mechanism with the hereditary transfer of carbon atoms and alloying elements, as well as defects in the crystal structure, to austenite from the original martensite.

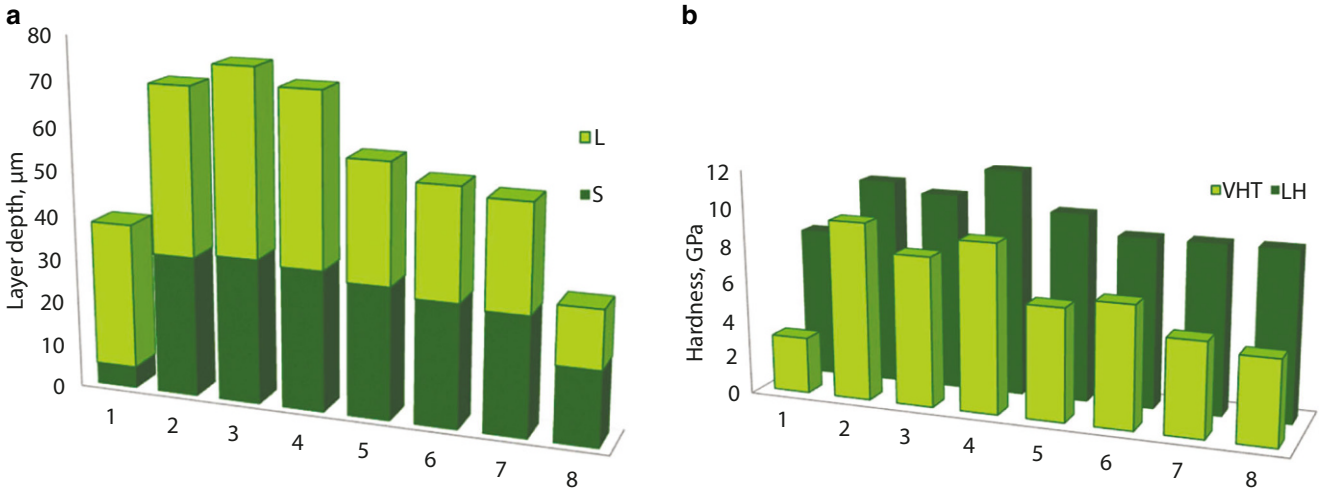

Fig. 10 Effect of the mode of volumetric heat treatment of R6M5 steel on the depth (**a**) and hardness (**b**) of the irradiated layer: *1* annealing; *2* hardening without tempering; *3* hardening and tempering at 200 °C; *4* tempering at 550 °C; *5* tempering at 625 °C; *6* tempering at 650 °C; *7* tempering at 700 °C; *8* 2 tempering treatments at 550 and 700 °C (S—laser hardening from the solid state, L—from the liquid state; VHT—volumetric heat treatment, LH—laser hardening)

Fig. 11 The hardness of steels after volumetric and laser processing depends on the dispersion of carbides

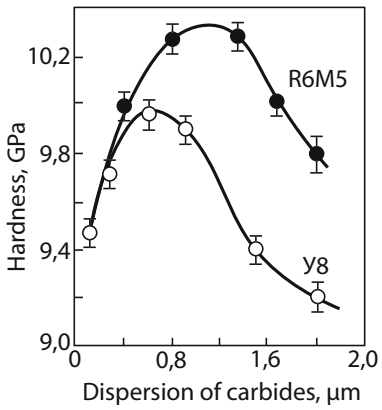

- High-temperature laser-hardened austenite has a fragmented structure with subgrains in sizes of 200–300 nm. This feature is explained by the dynamic polygonization of austenite, which occurs because of the superposition of dynamic thermostrictive effects in the laser processing zones on phase hardening during the α→γ transition.
- After high-speed cooling, the irradiated zones contain hereditary fine-needle martensite with a high level of strength, a certain amount of textured retained austenite, and a carbide phase.
- It has been established that the hardening of irradiated steel, which occurs under conditions of thermal deformation action of laser radiation, is associated, among other things, with the formation of nanosized zones with a dispersed structure and increased hardness (10–12 GPa) at the boundaries of the carbide steel matrix composition. According to the results of metallophysical and urometric studies, it was established that the maximum hardness of laser-hardened steels is achieved if dispersed carbides occupy more than 40% of the irradiated area and have dimensions of 0.5–1.5 μm.
- A reasonable choice of the initial steel structure and laser processing mode has been shown to enable obtaining a structural state of surface layers with high and predictable performance properties on the working surfaces of products.

References

1. Li X, Gua Y (2020) Theoretical fundamentals of short pulse laser-metal interaction: a review. Nanotechn Precis Eng 3:105–125
2. Gabdrakhmanov A, Galiakbarov A, Gaisin I (2019) Increasing efficiency of the laser action to materials. Mater Today: Proc 19:1965–1967
3. Roy S, Zhao J, Shrotriya P, Sundararajan S (2017) Effect of laser treatment parameters on surface modification and tribological behavior of AISI 8620 steel. Tribol Int 112:94–102
4. Aung-Ngwe T, Kim VA (2019) Dissipative structure of interaction of laser radiation with construction steel 45. Mater Today: Proc 19:2224–2229
5. Gubenko SI (1989) The dynamic nature of steel recrystallization under laser irradiation. MiTOM 10:2–5
6. Lu G, Sokol DW, Zhang Y, Dulaney JL (2019) Nanosecond pulsed laser-generated stress effect inducing macro-micro-nano structures and surface topography evolution. Appl Mater Today 15:171–184
7. Bernstein ML (1977) Structure of deformed metals. Metallurgiya, Moscow
8. Smithles KJ (1980) Metals: a reference book. Metallurgiya, Moscow
9. Yakovleva IL, Schastlivtsev VM, Tabatchikova TI (1995) Martensite-like diffusion-free shear mechanism of austenite formation during laser heating of steel with a pearlite structure. FMM 79(5):152–159
10. Sadovsky VD, Schastlivtsev VM, Tabatchikova TI (1987) Formation of austenite during ultrafast laser heating of steels with a massive martensite structure. FMM 63(3):555–561
11. Bernstein ML, Kaputkina LM, Prokoshkin SD (1982) Structure and substructure of austenite formed during heating of hardened and thermomechanically hardened steels. FMM 53(6):1143–1152
12. Sadovsky VD (1983) Transformations when heating steel. Structural heredity. In: Metallurgy and heat treatment of steel: a reference book. Metallurgiya, Moscow, pp 83–111
13. Dyachenko SS (2000) Heredity during phase transformations: mechanism of the phenomenon and influence on properties. MiTOM 4:14–19
14. Pustovoit VN, Dombrovskii YM, Dolgachev YV (2017) Structural identification of the phenomenon of 'White Zone. Met Sci Heat Treat 59:3–7
15. Brover GI, Shcherbakova EE (2023) Evolution of steel surface layer structure and properties during pulsed laser processing. Metallurgist 67(1/2):182–190
16. Tabatchikova TI (2008) Recrystallization and the possibility of implementing diffusion-free $\alpha \rightarrow \gamma$ -transformation during ultrafast laser heating of steels. FMM 105(3):294–318
17. Brover AV, Brover GI, Dyachenko LD (2007) Some features of the structural state of steels in laser processing zones. Izv Vyssh Ucheb Zav Chern Metall 6:37–40
18. Hongyu C, Dongdong G, Konrad K (2020) Laser additive manufactured high-performance Fe-based composites with unique strengthening structure. Mater Sci Tech 89:242–252
19. Kürnsteiner P, Wilms MB, Weisheit A, Barriobero-Vila P (2017) Massive nanoprecipitation in an Fe-19Ni-xAl maraging steel triggered by the intrinsic heat treatment during laser metal deposition. Acta Mater 4:52–60
20. Mirzababaei M, Pasebani S (2020) Selective laser melting and tempering of H13 tool steel for rapid tooling applications. J Alloys Compd 849:5543–5549

Authors and Affiliations

G. I. Brover[1] · E. E. Shcherbakova[1]

✉ G. I. Brover
abrover@mail.ru

E. E. Shcherbakova
bsherbakovaee@mail.ru

[1] "Materials Science and Metal Technologies" Department, Don State Technical University, Rostov-on-Don, Russian Federation